

Few-Shot Domain Adaptation for Learned Image Compression

Tianyu Zhang, Haotian Zhang, Yuqi Li, Li Li, Dong Liu

Abstract—Learned image compression (LIC) has achieved state-of-the-art rate-distortion performance, deemed promising for next-generation image compression techniques. However, pre-trained LIC models usually suffer from significant performance degradation when applied to out-of-training-domain images, implying their poor generalization capabilities. To tackle this problem, we propose a few-shot domain adaptation method for LIC by integrating plug-and-play adapters into pre-trained models. Drawing inspiration from the analogy between latent channels and frequency components, we examine domain gaps in LIC and observe that out-of-training-domain images disrupt pre-trained channel-wise decomposition. Consequently, we introduce a method for channel-wise re-allocation using convolution-based adapters and low-rank adapters, which are lightweight and compatible to mainstream LIC schemes. Extensive experiments across multiple domains and multiple representative LIC schemes demonstrate that our method significantly enhances pre-trained models, achieving comparable performance to H.266/VVC intra coding with merely 25 target-domain samples. Additionally, our method matches the performance of full-model finetune while transmitting fewer than 2% of the parameters.

Index Terms—Learned Image Compression, Domain Adaptation, Few-Shot Learning.

I. INTRODUCTION

With the explosion of images in modern multimedia, image compression has become crucial for efficient storage and transmission. Over the past decade, conventional standards including JPEG [45], H.265/HEVC [41] and H.266/VVC [9], have significantly contributed to the real-world applications of image compression. Recently, learned image compression (LIC) has made remarkable strides in rate-distortion (RD) performance by leveraging non-linear transforms and end-to-end optimization. Several studies [19; 30; 21] have even surpassed VTM (the reference software for H.266/VVC) on both peak signal-to-noise ratio (PSNR) and multi-scale structural similarity (MS-SSIM), indicating the immense potential of LIC for next-generation image compression techniques.

Despite the encouraging progress, some studies [38; 32; 42] have pointed out the performance degradation of pre-trained LIC models on out-of-domain images (we simplify in/out-of-training-domain as in/out-of-domain for convenience). It is common practice to train and evaluate LIC models on natural image benchmarks such as DIV2K [1], Kodak [16], Tecnick [2], and CLIC [12]. However, practical codecs may well be challenged by images from various domains, many of which have significant domain gaps compared to natural images. For demonstration purposes, we test advanced LIC models including Cheng2020 [11], ELIC [19], TCM [30], and MLIC++ [21] in Fig. 1. While all these models perform

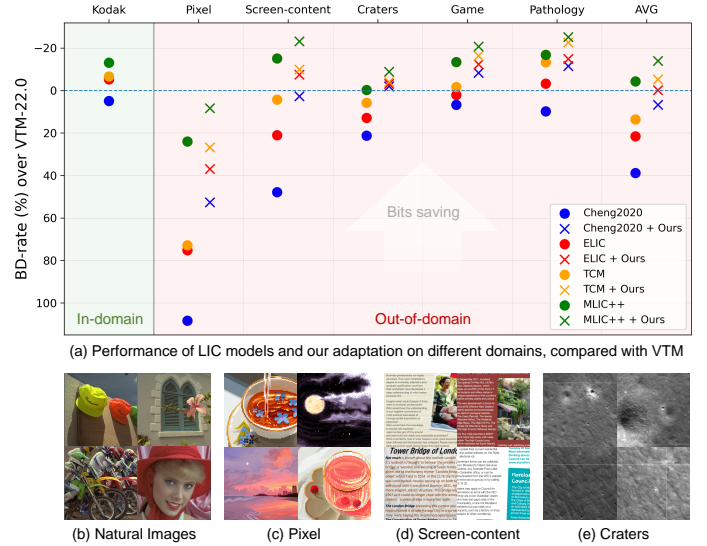


Fig. 1. (a) BD-rate (\downarrow) of four advanced LIC models with or without our method on different domains. (b)-(e) Images from different domains have visible different characteristics.

comparably or better than the conventional codec VTM on natural images, they exhibit varying degrees of performance drop and generally fall behind VTM on out-of-domain images such as pixel-style art and screen content, highlighting the necessity for efficient adaptation methods for pre-trained LIC models.

In this regard, most existing methods [38; 32; 42] suggest instance adaptation (IA), which aims to adapt LIC models to a single image at inference. Despite its effectiveness, IA does not perform actual domain adaptation (DA) for pre-trained models, and is time-consuming and computationally expensive due to its per-image online training. On the other hand, Katakol et al. [24] proposed DA for LIC using limited target samples. They suggested selective finetune, and adapted pre-trained models to a target domain with one-time training and transmission, demonstrating great adaptation efficiency for deployed models. Nevertheless, the proposed method is restricted to GDN structures [3], and suffers from large additional parameters on recent schemes [19; 30; 22].

Despite the promising applications like codec calibration for batch transmission, DA for LIC remains largely unexplored. Recently, Presta et al. [35] pre-trained a gate network on multiple domains, enhancing the generalization capacity of LIC models. However, they did not address the problem of adapting LIC models to a specific domain. Therefore, in this

paper, we focus on **adapting pre-trained LIC models to a target domain**. For practicality, we follow Katakol et al. [24] and study DA for LIC with limited samples. We also highlight the versatility of the DA method to different domains and mainstream LIC schemes.

Building on these insights, we propose a universal few-shot domain adaptation method for LIC using compact adapters, achieving superior performance across various domains and mainstream LIC schemes. Inspired by [28], we explore domain gaps in LIC through disturbed channel-wise decomposition. We demonstrate that pre-trained LIC models suffer from scattered channel-wise energy allocation on out-of-domain images. To address this problem, we introduce convolution-based adapters (Conv-Adapters) and low-rank adapters (LoRA-Adapters) to the pre-trained models for channel-wise re-allocation. These adapters are trained with a few target samples, and are plug-and-play for processing specific domains.

Our main contributions can be summarized as follows:

- We propose a universal few-shot domain adaptation method for learned image compression by incorporating compact adapters. Our method is applicable to different domains and mainstream LIC schemes.
- We explore the domain gaps in LIC through disturbed channel-wise decomposition, which results in scattered energy allocation on out-of-domain images. The proposed channel-wise re-allocation with adapters strengthens energy compaction.
- Extensive experiments verify the effectiveness of our method across mainstream domains and LIC schemes. We generally enhance pre-trained models to VTM on every domain, achieving comparable improvements to full-model finetune with tiny additional parameters.

II. RELATED WORK

A. Learned Image Compression

Learned image compression (LIC) has demonstrated competitive potential against traditional codecs. Ballé et al. [4] proposed the first end-to-end LIC model with non-linear transforms and uniform quantizer, which was further strengthened by hyperprior [5] and context model [33]. Cheng et al. [11] first achieved comparable performance with VTM using Gaussian mixture likelihoods. He et al. [19] proposed uneven channel autoregressive model, demonstrating pleasant performance and complexity. Recently, Liu et al. [30] designed Transformer-CNN mixture block to incorporate the ability of both structures for LIC. Jiang et al. [22] introduced multi-reference context to capture different correlations, achieving the state-of-the-art performance [21].

In the regard of interpretability, early work [5; 11] visualized the latent in LIC to evaluate the preciseness of the entropy model. He et al. [19] sorted latent channels by energy, suggesting low-frequency components concentrated on a few channels while the rest was extremely sparse. Duan et al. [14] interpreted latent channels as orthogonal transform coefficients, while Li et al. [28] suggested frequency decomposition is an intrinsic property for LIC. Nevertheless, these results on latent representation did not fully consider out-of-domain images.

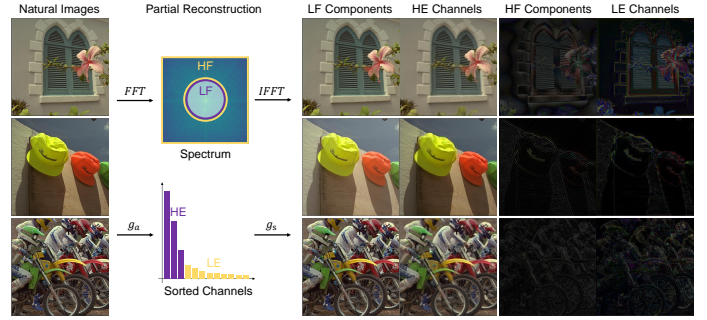


Fig. 2. Analogy between frequency components and channels of LIC latents. For one image, we perform Fast Fourier Transform (FFT) and then reconstruct from low-frequency (LF) or high-frequency (HF) components respectively. Similarly, we perform a learned analysis transform (g_a) and then reconstruct from high-energy (HE) or low-energy (LE) channels respectively. Please view on screen and zoom in to observe the reconstructions from HF/LE.

B. Adaptation for Learned Image Compression

To alleviate domain gaps in LIC, two kinds of adaptation namely instance adaptation (IA) and domain adaptation (DA) have been studied for LIC. IA [10; 43; 42; 38; 32] adapts pre-trained models to a single image rather than a domain using per-image online training, including content [49; 10] and decoder [44; 43; 51; 42; 38; 32] adaptation. The additional parameters are compressed and transmitted together with bitstream. Despite its effectiveness, IA is computationally expensive and time-consuming due to its per-image fashion.

Contrary to IA, Katakol et al. [24] introduced the problem of DA for LIC, adapting pre-trained LIC models to a target domain using multiple samples and one-time training. They suggested finetuning GDN layers [3] with channel-wise parameters and the entire entropy model. However, this is restricted by specific network structures, and additional parameters due to the complex entropy models. We alleviate this issue by designing compact and universal adapters.

The scope of this work belongs to DA, which is distinct from IA on several dimensions: (a) Our goal is transferring pre-trained LIC models to a target domain rather than a specific instance. Besides, (b) our method adopts one-time training and transmission rather than the per-image fashion at inference. The additional parameters are evaluated alone and are independent to bitstream and bit-rate. In addition, we suggest this work is complementary to instance adaptation, as we demonstrate the compatibility of both techniques for further RD improvement on out-of-domain images.

C. Few-Shot Domain Adaptation

Domain adaptation [37; 39] aims to bridge the gap between the source domain and the target domain, which exists widely in deep learning. In practice, collecting sufficient data from a specific domain can be expensive and difficult due to various limitations. Therefore, the combination of few-shot learning [15; 40] and domain adaptation plays a critical role. Adapting on a few target samples, models pre-trained on a source domain are expected to perform similarly on a target domain [27]. Although few-shot domain adaptation has been well explored in many computer vision tasks, like

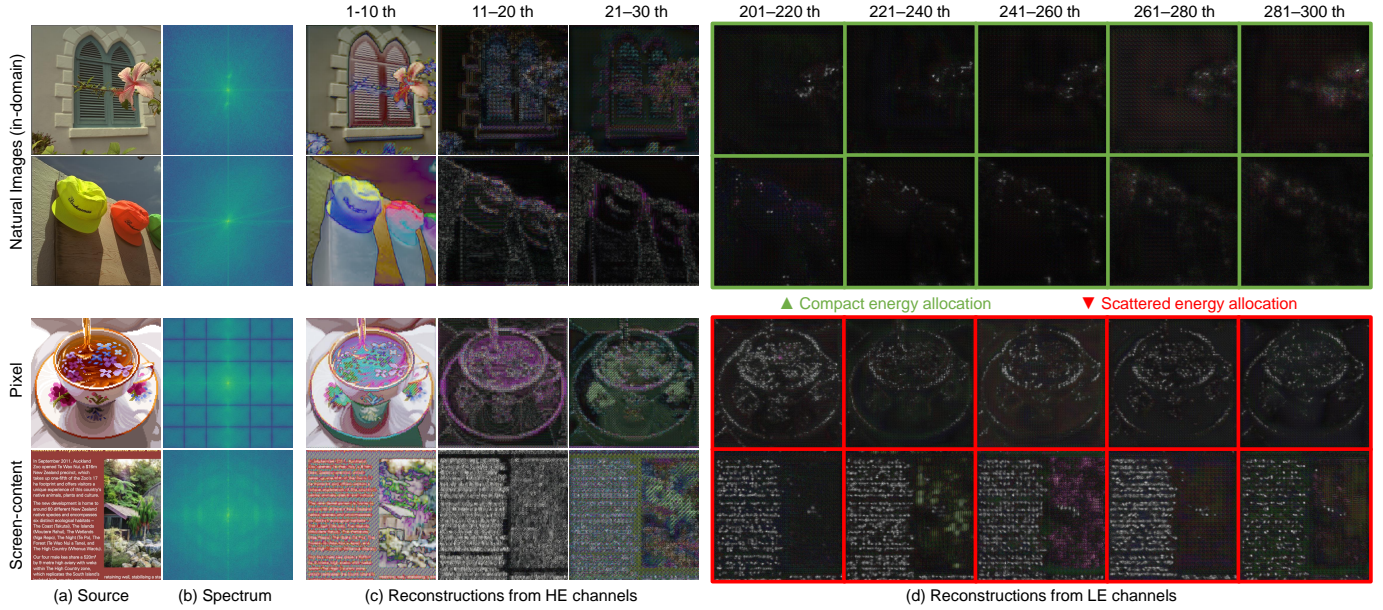


Fig. 3. Following Fig. 2, we explore the domain gaps by observing the channel-wise decomposition. The top two rows display in-domain natural images, while the bottom two rows show out-of-domain images. (a) Source image. (b) Spectrum (using FFT). (c, d) Reconstructions from different HE channels and LE channels respectively. Here the total number of channels is 320. *Out-of-domain images have more HF components as shown in (b), as well as more information embedded into LE channels as shown in (d). Thus, our key idea is to re-allocate the information from LE channels to HE channels for out-of-domain images.*

image classification [29; 13], segmentation [25; 31; 23], and generation [17; 26; 50; 46], limited attention has been paid to learned image compression, and there still lack universal few-shot domain adaptation methods for mainstream learned image compression schemes and domains.

III. METHOD

A. Motivation

Recent studies [14; 28] suggest that the transform in LIC can be interpreted as channel-wise frequency decomposition in a non-linear fashion. We compare latent channels to frequency components of a source image using linear transforms (e.g. FFT), as reconstructions from partial channels or partial frequency components demonstrate obvious similarities in Fig. 2. Motivated by this, we further study the channel-wise decomposition on different domains by reconstructions from specific channels in Fig. 3 (c) and (d). Consistent with previous findings [19; 14; 28], decomposed information concentrates on high-energy channels (respectively low-frequency). For in-domain images, the energy allocation on channels is more compact, with little information of the source images found in low-energy channels. However, for out-of-domain images, more high-frequency components are presented in the spectrum (Fig. 3 (b)), and obvious contours of source images can be observed in reconstructions from low-energy channels, as shown in Fig. 3 (d). This indicates a scattered energy allocation of the pre-trained LIC model on out-of-domain images, which differs from the compact energy allocation on in-domain images.

Given these channel-wise differences among latents of in-domain and out-of-domain images, we assume that the following entropy estimation and reconstruction modules can not op-

erate effectively in the pre-trained manner due to improper latents, leading to degraded rate-distortion performance. Therefore, our key idea is to perform channel-wise re-allocation, which concentrates the information from LE channels to HE channels for out-of-domain images. Specifically, we propose gently re-allocating the channels of intermediate latents by inserting compact adapters into the pre-trained models. The implementation and performance of these adapters are detailed in the following sections.

B. Channel-wise Re-allocation with Adapters

We present the deployment of our method on ELIC [19] in Fig. 4. Two types of adapters, namely Conv-Adapters and LoRA-Adapters, are introduced. To refine the channel-wise decomposition in the transform, we insert Conv-Adapters after non-linear blocks. For entropy estimation, LoRA-Adapters are applied to the entropy parameters network. We highlight the compatibility of the proposed method to mainstream schemes.

1) *Conv-Adapters*: We introduce Conv-Adapters to the transform to adjust the channels of intermediate latents. Denoting the output latent of a specific block as $L \in \mathbb{R}^{c \times h \times w}$ and its i th channel $L_i \in \mathbb{R}^{h \times w}$, we aim to re-allocate the information on channels before passed to the next block:

$$L' = (L'_0, L'_1, \dots, L'_{c-1}) = f(L_0, L_1, \dots, L_{c-1}) \quad (1)$$

where L' denotes the output latent with refined information allocation on channels, and f denotes the re-allocation mechanism introduced by Conv-Adapters. Considering the restriction on computational complexity and limited samples, we simplify this mechanism into a channel-wise linear transform, and apply $\text{Conv}1 \times 1$ as the Conv-Adapter. To maintain the training stability, we initialize the weight matrix $W \in \mathbb{R}^{c \times c \times 1 \times 1}$ of

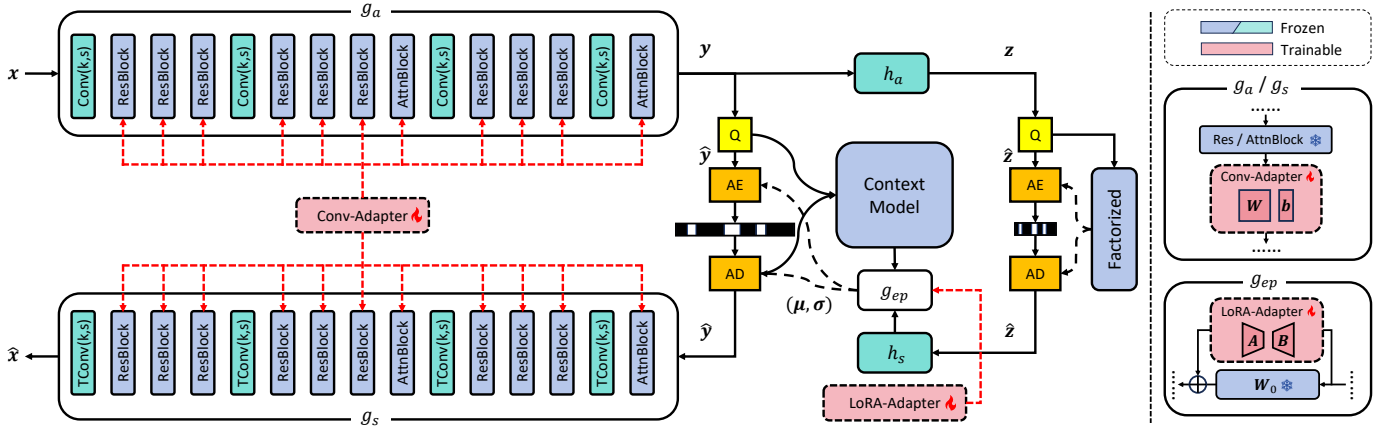


Fig. 4. Deployment of our method on ELIC [19]. We denote g_{ep} as the entropy parameters network, while the other notations follow the same explanations in [19]. As detailed on the right, Conv-Adapters are inserted serially after non-linear blocks in the transform, while LoRA-Adapters are added to the pre-trained weight matrix W_0 in g_{ep} . W and b are weight and bias of Conv-Adapter, respectively, while A and B are low-rank matrices. Only adapters are trainable.

$\text{Conv}1 \times 1$ to identity matrix $I \in \mathbb{R}^{c \times c \times 1 \times 1}$, and the bias $b \in \mathbb{R}^c$ to zeros. Therefore, we refine intermediate latents in the transform by the following linear re-allocation:

$$L' = W \cdot (L_0, L_1, \dots, L_{c-1})^T + b \quad (2)$$

2) *LoRA-Adapters*: To accommodate the channel-wise re-allocation in the transform, we adopt Low-Rank Adaptation (LoRA) [20; 32] in the entropy model. Mainstream LIC schemes have large variances on the entropy model, resulting in difficulty for a universal adaptation method on entropy estimation. Besides, hidden dimensions in the entropy model are empirically large for better performances, indicating convolution-based adapters will boost the amount of additional parameters. Therefore, we introduce low-rank matrices (LoRA-Adapters) to the common entropy parameters network. Namely, we modify the weight of a pre-trained layer $W_0 \in \mathbb{R}^{c_{out} \times c_{in} \times h \times w}$ by:

$$\begin{aligned} W'_0 &= W_0 + \Delta W \\ \Delta W &= BA \end{aligned} \quad (3)$$

where $A \in \mathbb{R}^{r \times c_{in}}$ is initialized with Gaussian, $B \in \mathbb{R}^{c_{out} \times r}$ is set to zeros, ensuring $\Delta W = 0$ thus the training stability. The rank $r \ll \min\{c_{in}, c_{out}\}$, and is set to 10 empirically. LoRA-Adapters serve as bias on channel dimension for pre-trained weights, and can be merged once trained without introducing additional latency at inference.

C. Two-Stage Training Strategy

The training of adapters consists of two stages, as detailed in Fig. 4 and Fig. 5 respectively. We denote $\theta = \{W, b, A, B\}$ as the total parameters of adapters. Given the analysis transform g_a , synthesis transform g_s , hyper analysis transform h_a , uniform scalar quantization Q , and λ to balance bit-rate \mathcal{R} and distortion \mathcal{D} , we first freeze all pre-trained parameters ϕ and train adapters θ jointly with:

$$\mathcal{L}(\theta) = \mathcal{R}(\hat{y}) + \mathcal{R}(\hat{z}) + \lambda \cdot \mathcal{D}(x, \hat{x}) \quad (4)$$

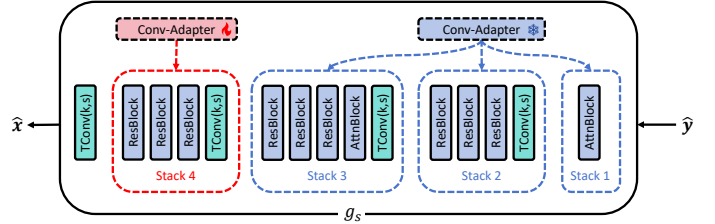


Fig. 5. Division of g_s into four stacks. In the second stage, we only finetune adapters in Stack 4 for reconstruction.

where:

$$\begin{aligned} \hat{y} &= Q(g_a(x; \phi, \theta)) \\ \hat{x} &= g_s(\hat{y}; \phi, \theta) \\ \hat{z} &= Q(h_a(y; \phi)) \end{aligned} \quad (5)$$

We suggest adapters optimized by a joint objective function suffer from insufficient training under limited samples. Inspired by the two-stage training strategy in [18], we further conduct a second training stage. Concretely, we divide g_s into four stacks by upsample operations, as shown in Fig. 5. We freeze all the adapters except the ones in Stack 4, and finetune this small set (denoted as $\Delta\theta$) with hard quantization and distortion only:

$$\mathcal{L}(\Delta\theta) = \mathcal{D}(x, \hat{x}), \text{ switch } Q \text{ to rounding.} \quad (6)$$

We demonstrate in Section 4.3 that this stage is simple but effective without introducing more parameters. Once trained, adapters in g_a are stored at the encoder, while the rest should be transmitted to the decoder. In this way, a full set of adapters corresponds to a certain domain, and is plug-and-play for flexibly processing specific domains.

IV. EXPERIMENTS

A. Settings

1) *Domains and Datasets*: We follow Lv et al. [32]; Shen et al. [38] and sort five domains with 150 images each, including (i) pixel-style images [32]; (ii) screen content images

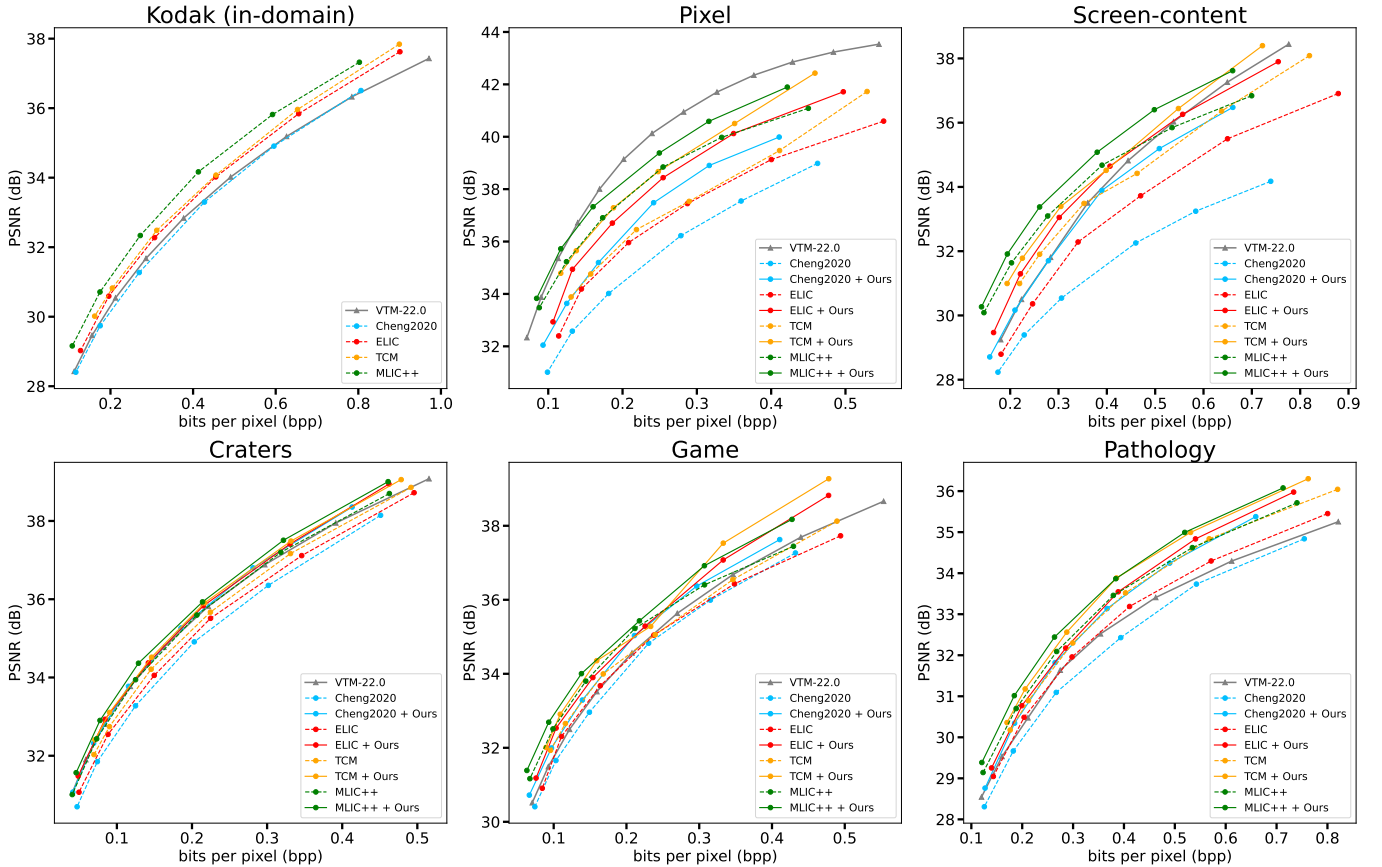


Fig. 6. RD curves including VTM-22.0 intra coding, pre-trained LIC models, and models adapted with 25 samples in our method. We generally enhance pre-trained models to the level of VTM on the other five domains.

from SCID [34], SCI1K [48], SIQAD [47]; (iii) craters images cropped from Lunar Reconnaissance Orbiter Camera (LROC) [36]; (iv) game images cropped from GamingVideoSET [6]; (v) pathology images cropped from BRACS [8]. All crops have the same resolution of 600×800 . We select a fixed test set with 100 images for each domain. Besides, we use Kodak to represent the natural image domain.

2) *Models*: We test our method on advanced LIC models, namely Cheng2020 [11], ELIC [19], MLIC++ [21] and TCM [30]. We use the official pre-trained weights except ELIC, for which we train ourselves for a lack of official weights.

3) *Implementation*: We train adapters with $N = \{5, 10, 25\}$ samples, respectively. We split the samples into training and validation set in a proportion of 4:1. We use a patch size of 256 and a batch size of 4. In the first stage, we set learning rate stages $\{50, 10, 7.5, 5, 2.5, 1\} \times 10^{-5}$. For different N , we further set max epoch = $\{250, 500, 750\}$. In the second stage, we train selected adapters for another max epoch with fixed learning rate 5×10^{-4} .

B. Adaptation Performance

1) *Comparisons with Traditional Codec*: We compare the proposed method with the conventional standard VVC by VTM-22.0 intra coding. We plot the rate-distortion (RD) curves on Kodak (in-domain) and the other five domains in Fig. 6. All pre-trained models perform comparably or better

TABLE I
THE NUMBER OF ADDITIONAL PARAMETERS TO TRANSMIT COMPARED WITH FULL-MODEL FINETUNE AND DANICE [24], NOTE THAT DANICE CAN NOT BE APPLIED TO ELIC.

Baseline	Params	Method	Transmit	Prop.
Cheng2020	31.48M	Finetune	24.12M	76.62%
		DANICE	10.86M	34.50%
		Ours	0.37M	1.17%
ELIC	40.72M	Finetune	30.98M	76.08%
		DANICE	/	/
		Ours	0.71M	1.74%
TCM	45.18M	Finetune	41.93M	92.81%
		DANICE	35.17M	77.84%
		Ours	0.88M	1.95%
MLIC++	116.72M	Finetune	110.45M	94.71%
		DANICE	98.41M	84.31%
		Ours	0.73M	0.63%

TABLE II
COMPUTATIONAL COMPLEXITY COMPARISONS OF THE PROPOSED METHOD AND DIFFERENT SOURCE MODELS. THE RESULTS ARE AVERAGED ON KODAK WITH A SINGLE TESLA V100 GPU.

Baseline	Dec. T (s)		MFLOPs / pixel	
	Source	Ours	Source	Ours
Cheng2020	9.570	9.588 $_{+0.19\%}$	1.03	1.08 $_{+5.21\%}$
ELIC	0.319	0.324 $_{+1.50\%}$	0.85	0.92 $_{+9.22\%}$
TCM	0.269	0.270 $_{+0.60\%}$	0.54	0.58 $_{+7.07\%}$
MLIC++	0.338	0.342 $_{+1.30\%}$	1.26	1.31 $_{+3.90\%}$

TABLE III

DETAILED BD-RATE (\downarrow) USING DIFFERENT NUMBERS OF TARGET SAMPLES (N) FOR DOMAIN ADAPTATION. WE COMPARE OUR METHOD WITH FULL-MODEL FINETUNE AND DANICE [24]. THE ANCHORS ARE CORRESPONDING PRE-TRAINED MODELS. NOTE THAT DANICE CAN NOT BE APPLIED TO ELIC AS GDN IS NOT USED.

N	Baseline	Method	Pixel	Screen-content	Craters	Game	Pathology	AVG
5	Cheng2020	Finetune	-23.09%	-25.51%	4.35%	-10.69%	-16.49%	-14.29%
		DANICE	-4.92%	-4.48%	-7.31%	-2.65%	-5.62%	-5.00%
		Ours	-21.95%	-23.99%	-8.55%	-8.93%	-13.58%	-15.40%
	ELIC	Finetune	-15.82%	-15.82%	-3.26%	-2.73%	-9.57%	-9.44%
		DANICE	/	/	/	/	/	/
		Ours	-17.36%	-16.27%	-6.07%	-4.78%	-10.70%	-11.04%
	TCM	Finetune	-17.88%	-7.16%	-4.75%	-4.78%	-7.87%	-8.49%
		DANICE	-1.66%	-1.64%	-3.20%	-0.85%	-3.17%	-2.10%
		Ours	-20.10%	-6.61%	-3.31%	-4.23%	-9.40%	-8.73%
	MLIC++	Finetune	-3.23%	-3.09%	-1.24%	-3.31%	-6.93%	-3.56%
		DANICE	-0.60%	-0.33%	-2.63%	0.12%	-4.49%	-1.63%
		Ours	-9.84%	-5.41%	-1.62%	-2.46%	-8.13%	-5.49%
10	Cheng2020	Finetune	-27.76%	-28.42%	-16.79%	-13.48%	-17.48%	-20.79%
		DANICE	-8.19%	-7.78%	-10.88%	-4.50%	-7.14%	-7.70%
		Ours	-27.44%	-28.00%	-15.25%	-11.34%	-17.78%	-19.96%
	ELIC	Finetune	-20.84%	-21.92%	-13.06%	-9.25%	-10.41%	-15.10%
		DANICE	/	/	/	/	/	/
		Ours	-21.38%	-22.35%	-10.64%	-6.32%	-11.87%	-14.51%
	TCM	Finetune	-24.06%	-13.08%	-8.95%	-7.28%	-9.67%	-12.61%
		DANICE	-2.95%	-3.11%	-5.52%	1.35%	-3.67%	-2.78%
		Ours	-24.18%	-11.87%	-7.06%	-9.01%	-10.24%	-12.47%
	MLIC++	Finetune	-8.71%	-8.93%	-7.84%	-4.07%	-8.90%	-7.69%
		DANICE	-0.32%	-0.37%	-4.22%	1.52%	-4.97%	-1.67%
		Ours	-13.82%	-9.95%	-5.66%	-5.32%	-9.16%	-8.78%
25	Cheng2020	Finetune	-30.37%	-34.99%	-22.83%	-19.66%	-17.72%	-25.11%
		DANICE	-11.30%	-11.59%	-13.58%	-6.88%	-9.83%	-10.64%
		Ours	-27.85%	-31.10%	-19.12%	-14.20%	-18.52%	-22.16%
	ELIC	Finetune	-24.63%	-25.62%	-17.15%	-15.95%	-10.76%	-18.82%
		DANICE	/	/	/	/	/	/
		Ours	-23.35%	-24.95%	-13.77%	-13.83%	-12.29%	-17.64%
	TCM	Finetune	-28.76%	-15.53%	-13.16%	-12.03%	-10.21%	-15.94%
		DANICE	-4.12%	-4.81%	-8.52%	2.30%	-4.34%	-3.90%
		Ours	-27.82%	-13.81%	-8.96%	-14.86%	-10.71%	-15.24%
	MLIC++	Finetune	-12.97%	-9.78%	-11.82%	-10.61%	-9.35%	-10.91%
		DANICE	-0.61%	-0.79%	-7.15%	-0.01%	-4.90%	-2.69%
		Ours	-14.63%	-12.09%	-8.50%	-9.70%	-10.27%	-11.04%

than VTM on Kodak, but most of them fall behind VTM on the other five domains. Our method enhances these models to the level of VTM except on the Pixel domain, where the domain gap is too wide to fully compensate [32].

2) *Comparisons with Domain Adaptation Method:* To evaluate the efficiency, we also compare with existing DA method DANICE [24] and full-model finetune by RD performance and complexity. We demonstrate detailed adaptation results under different N by computing BD-rate [7] in Table III. It is noted that DANICE is restricted to GDN structures [3], making it inapplicable to baselines like ELIC. Additionally, DANICE fails to achieve domain adaptation in some conditions, such as TCM and MLIC++ on the Game domain, indicating a limited versatility. Our method, however, achieves excellent adaptation performance in all conditions, performing comparably with full-model finetune and significantly outperforming DANICE.

In the regard of complexity, we highlight the compactness of the proposed adapters in Table I and Table II. Our method only needs to transmit fewer than 2% of the total parameters, while much more parameters need considering in DANICE and finetune due to the complex entropy model. Besides, we examine the variations in decoding time and FLOPs introduced by the proposed adapters in Table II. Our method increase FLOPs by less than 10% and coding time by less than 1.5%.

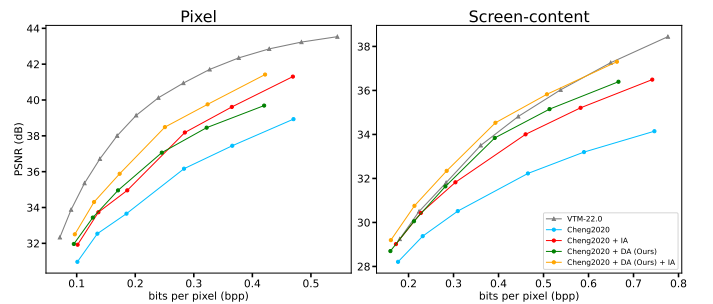


Fig. 7. Compatibility between our method and representative instance adaptation method [32] (abbreviated as DA and IA, respectively). We plot the rate-distortion curves on the Pixel and Screen-content domain.

3) *Comparisons with Instance Adaptation Method:* We compare our proposed domain adaptation (DA) method for LIC with existing instance adaptation (IA) methods [10; 43; 42; 38; 32]. IA adapts a pre-trained LIC model to individual images through per-image online training during inference. In contrast, DA involves a one-time training process on multiple images, adapting the model to a target domain before inference. Consequently, we suggest that our proposed DA method for LIC complements existing IA methods. The compatibility

TABLE IV
ABLATION STUDIES CONDUCTED ON ELIC ADAPTED WITH 25 SAMPLES. THE ANCHOR OF BD-RATE (\downarrow) IS PRE-TRAINED ELIC MODELS.

Stage 1		Stage 2		Pixel	Screen-content	Craters	Game	Pathology	AVG
Conv	LoRA	Stack	Stack 1234						
✓				-19.38%	-23.73%	-10.84%	-12.73%	-10.30%	-15.40%
✓	✓			-20.40%	-24.28%	-12.57%	-13.40%	-11.50%	-16.43%
✓	✓		✓	-19.92%	-22.46%	-11.95%	-10.68%	-10.95%	-15.19%
✓	✓			✓	-23.35%	-24.95%	-13.77%	-13.83%	-17.64%

TABLE V
EXPLORATIONS ON THE STRUCTURES OF CONV-ADAPTERS. EVALUATED BY THE PARAMETERS TO TRANSMIT AND THE BD-RATE (\downarrow).

Structure	Pixel	Screen-content	Craters	Game	Pathology	AVG	Transmit
GDN	-7.69%	-9.93%	-7.85%	-3.38%	-7.99%	-7.37%	0.26M
Depthwise Conv3×3	-11.31%	-15.41%	-9.98%	-5.42%	-11.06%	-10.63%	0.26M
Depthwise Conv3×3 + Conv1×1	-20.86%	-24.02%	-13.15%	-11.40%	-12.53%	-16.39%	0.73M
Conv3×3	-22.49%	-24.44%	-13.32%	-15.11%	-11.60%	-17.39%	4.48M
Conv1×1 (Ours)	-23.35%	-24.95%	-13.77%	-13.83%	-12.29%	-17.64%	0.71M

TABLE VI
EXPLORATIONS ON THE DEPLOYMENT OF CONV-ADAPTERS. EVALUATED BY THE PARAMETERS TO TRANSMIT AND THE BD-RATE (\downarrow).

Stack 1	Stack 2	Stack 3	Stack 4	Pixel	Screen-content	Craters	Game	Pathology	AVG	Transmit
✓				-4.89%	-4.89%	-6.64%	-2.65%	-8.24%	-5.46%	0.34M
✓	✓			-6.70%	-7.44%	-7.83%	-3.81%	-10.23%	-7.20%	0.45M
✓	✓	✓		-12.23%	-14.48%	-10.64%	-6.96%	13.48%	-11.56%	0.60M
✓	✓	✓	✓	-23.35%	-24.95%	-13.77%	-13.83%	-12.29%	-17.64%	0.71M

between these methods is illustrated in Fig. 7.

Specifically, we explore the combination of our proposed method with one of the latest IA methods [32]. We apply both techniques to the Pixel and Screen-content domain. For alignment, we use the pre-trained Cheng2020 model [11] as the baseline. Our DA method is conducted with 25 target samples, followed by implementing IA for each image on the adapted model. The rate-distortion curves, compared with VTM-22.0 intra coding, the pre-trained Cheng2020, and each technique individually, are shown in Fig. 7. Note that some curves differ slightly due to the different padding method adopted by Lv et al. [32] in their released code; we respect their implementation in Fig. 7. When combining both techniques, the RD performance is further improved, indicating that our method complements IA by introducing additional domain information from a limited number of samples.

Regarding encoding complexity, IA relies on expensive per-image online training, whereas DA is more efficient due to its one-time training on multiple samples. We display the encoding time for processing different numbers of test images in Fig. 8. For DA, a fixed one-time training is required to adapt the pre-trained LIC model to the target domain. Adapting the pre-trained Cheng2020 model with 25 samples takes less than half an hour on a single Tesla V100 GPU. Once adapted, the model achieves similar encoding speed on test images as the source model. In contrast, IA requires time-consuming online training for every test image, resulting in a significantly longer per-image encoding time compared to the source model. Therefore, DA is considerably more efficient than IA when encoding a batch of target-domain images.

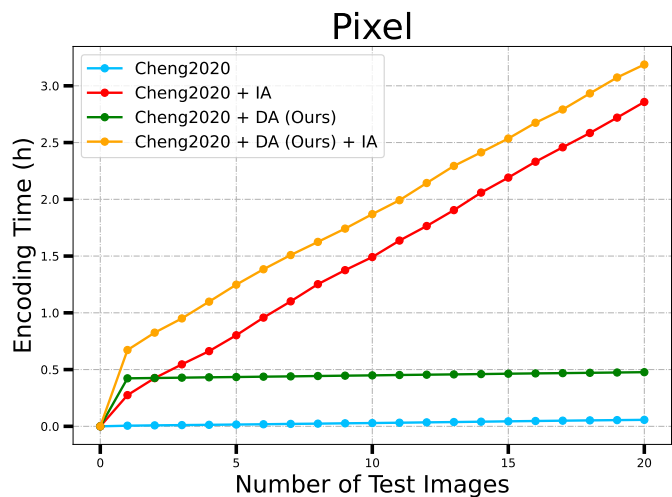


Fig. 8. Encoding time of different adaptation methods when applied to different numbers of test images from the Pixel domain, using a single Tesla V100 GPU. The proposed few-shot domain adaptation method is conducted on 25 target samples.

C. Ablation Studies

We conduct ablation studies to evaluate the contributions of Conv-Adapters, LoRA-Adapters and the two-stage training strategy. Using pre-trained ELIC as the baseline, we perform the proposed adaptation with 25 samples on the five domains. The results are shown in Table IV. Conv-Adapters achieve an average reduction of 15.40% in BD-rate compared to pre-trained models, while LoRA-Adapters and the two-stage training strategy each contributes an additional 1% BD-rate reduction. We also compare our second stage strategy with finetuning all Conv-Adapters in the decoder and display the

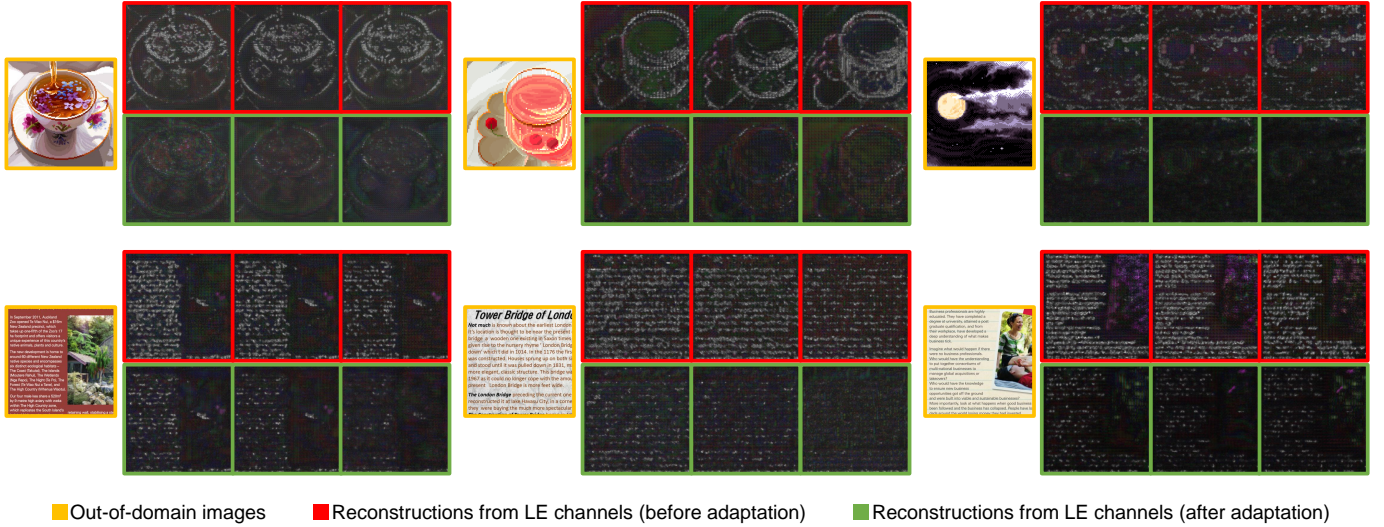


Fig. 9. Following Fig. 3, we display reconstructions from low-energy (LE) channels on out-of-domain images. The top row is Pixel, and the bottom row is Screen-content. As observed, our method efficiently reduces the information from LE channels.

superiority of our method.

Given that Conv-Adapter, which involves linear re-allocation on channels, has the most significant impact on adaptation performance, we further explore the structures of Conv-Adapters in Table V and the deployment strategy in Table VI. We conduct adaptation on ELIC using 25 target samples and evaluate the performance based on the parameters to transmit, and the BD-rate between the adapted model and the source model. Our results demonstrate the efficiency of our method in terms of both BD-rate and parameter requirements.

For the structures, we first replace the proposed $\text{Conv}1 \times 1$ with more compact structures such as GDN [3] and depthwise $\text{Conv}3 \times 3$. We then test more complex structures, including $\text{Conv}3 \times 3$ and a sequence of depthwise $\text{Conv}3 \times 3$ followed by $\text{Conv}1 \times 1$. For all structures, we follow the restriction on initialization and initialize them to perform identical transforms at the start of training. Using ELIC [19] as the baseline model, we conduct adaptation experiments on five domains, each with 25 target samples. The training strategy for adapters remains consistent. As shown in Table V, compact structures like GDN and depthwise $\text{Conv}3 \times 3$ have fewer parameters to transmit but exhibit significant degradation in average adaptation performance. For more complex structures, the increased parameters in the spatial dimension fail to further improve performance, underscoring the efficiency of $\text{Conv}1 \times 1$ in balancing complexity and performance.

For the deployment strategy, following Fig. 5, we divide the analysis transform and the synthesis transform into four stacks and gradually apply Conv-Adapters to each stack. Although the parameters to transmit increase, applying Conv-Adapters to all stacks significantly enhances adaptation performance. Therefore, we recommend deploying Conv-Adapters in all stacks. We visualize the kernels after training in Fig. 10.

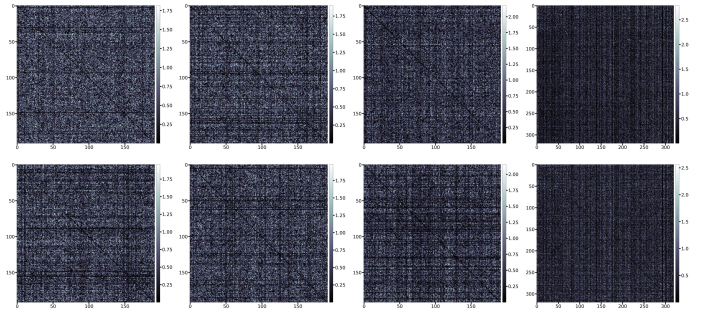


Fig. 10. Visualization of Conv-Adapter kernels after training. Four pairs of kernels symmetrical in transform are displayed in two rows, where the top row comes from g_a and the bottom row comes from g_s . We find obvious relevance on rows and columns of the kernels, suggesting channel-wise correlations remain in the latents have been captured.

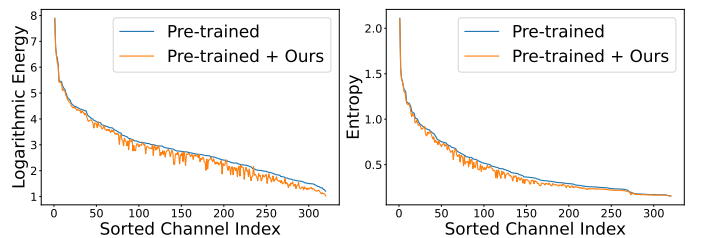


Fig. 11. Distributions of energy and entropy on channels. The channels are sorted by the distributions of pre-trained models. The results are averaged on the Pixel domain.

D. Analyses on Channel-wise Re-allocation

We propose channel-wise re-allocation with adapters in the pre-trained LIC model for domain adaptation. We get motivated by the observation that the pre-trained channel-wise decomposition is disturbed by out-of-domain images, resulting in scattered energy allocation across channels. To highlight this issue and demonstrate the effectiveness of our method, we

perform detailed analyses focusing on the channels of latent representation. We conduct experiments on pre-trained ELIC models. We perform the proposed method on the Pixel domain using 25 target samples.

1) *Variation on Channels*: We use the output latent of the analysis transform, and study the distribution of logarithmic energy and entropy on channels following [19] in Fig. 11. The results are averaged on the Pixel domain. We find that both energy and entropy on specific channels drop after adapting with adapters. Especially, the variation is more apparent on low-energy channels, while high-energy channels remain almost unchanged. This suggests that the energy becomes more concentrated to high-energy channels on out-of-domain images.

2) *Reconstructions from Low-Energy Channels*: To further investigate the variation on channel-wise decomposition, we compare the reconstructions from low-energy channels before and after adaptation. Concretely, we keep specific channels unchanged and mask the rest into zeros, reconstruct the modified latent, then subtract the reconstruction of all-zero one. We sort the channels by energy, and display the reconstructions from specific ranges of channels after 200th in Fig. 9, which is similar to Fig. 3. We find weaker details of inputs can be observed in reconstructions from the model adapted with our method, suggesting high-frequency components have been better moved out of the low-energy channels, which is more in line with the compact energy allocation in processing in-domain images. Thus, we suggest the pre-trained frequency decomposition on high-frequency components is strengthened by our method.

E. Visualization of Reconstructions

We present the qualitative reconstruction results of the pre-trained ELIC [19], the model adapted with our method using 25 samples, and the corresponding reconstruction errors in Fig. 12. The model is optimized using MSE with $\lambda = 0.483$. We showcase out-of-domain samples from the five domains we used: Pixel, Screen-content, Craters, Games, and Pathology. Specific 50×50 crops from the reconstructions are displayed with pixel enlargement for better visibility.

In addition to RD improvement, reconstructions from the model adapted with our method demonstrate superior visual quality, particularly in high-frequency edges and details. For Pixel and Screen-content samples, the sharp edges of pixel-style art and letters are reconstructed more accurately. For samples from Craters, Games, and Pathology, our reconstructions capture more details of the ground truth. Additionally, we compute the reconstruction errors relative to the ground truth, finding that our method primarily reduces reconstruction errors at edges and in fine details.

V. CONCLUSION

In this paper, we propose a universal few-shot domain adaptation method for learned image compression. With pleasant RD improvement and limited complexity, we expand the proposed method to multiple domains and multiple representative LIC schemes, demonstrating its versatility. We explore the domain gaps in LIC through disturbed channel-wise

decomposition, and introduce compact adapters for channel-wise re-allocation. With our method the domain adaptation of LIC models can be simplified into lightweight training, transmission, and storage of compact adapters, achieving flexibility and efficiency. We conduct sufficient experiments showing the proposed method enhances pre-trained models to the level of VTM generally, and significantly outperforms existing domain adaptation method. We hope our findings provide inspiration for future research on domain adaptation for LIC, thus contributing to the real-world deployment of versatile learned image compression.

REFERENCES

- [1] Eirikur Agustsson and Radu Timofte. Ntire 2017 challenge on single image super-resolution: Dataset and study. In *Proceedings of the IEEE conference on computer vision and pattern recognition workshops*, pages 126–135, 2017.
- [2] Nicola Asuni and Andrea Giachetti. Testimages: a large-scale archive for testing visual devices and basic image processing algorithms. In *STAG: Smart Tools & Apps for Graphics*, pages 63–70, 2014.
- [3] Johannes Ballé, Valero Laparra, and Eero P Simoncelli. Density modeling of images using a generalized normalization transformation. *arXiv preprint arXiv:1511.06281*, 2015.
- [4] Johannes Ballé, Valero Laparra, and Eero P Simoncelli. End-to-end optimized image compression. *arXiv preprint arXiv:1611.01704*, 2016.
- [5] Johannes Ballé, David Minnen, Saurabh Singh, Sung Jin Hwang, and Nick Johnston. Variational image compression with a scale hyperprior. *arXiv preprint arXiv:1802.01436*, 2018.
- [6] Nabajeet Barman, Saman Zadtootaghaj, Steven Schmidt, Maria G Martini, and Sebastian Möller. Gamingvideose: a dataset for gaming video streaming applications. In *2018 16th Annual Workshop on Network and Systems Support for Games (NetGames)*, pages 1–6. IEEE, 2018.
- [7] Gisle Bjontegaard. Calculation of average psnr differences between rd-curves. *ITU SG16 Doc. VCEG-M33*, 2001.
- [8] Nadia Brancati, Anna Maria Anniciello, Pushpak Pati, Daniel Riccio, Giosuè Scognamiglio, Guillaume Jaume, Giuseppe De Pietro, Maurizio Di Bonito, Antonio Foncubieta, Gerardo Botti, et al. Bracs: A dataset for breast carcinoma subtyping in h&e histology images. *Database*, 2022:baac093, 2022.
- [9] Benjamin Bross, Ye-Kui Wang, Yan Ye, Shan Liu, Jianle Chen, Gary J Sullivan, and Jens-Rainer Ohm. Overview of the versatile video coding (vvc) standard and its applications. *IEEE Transactions on Circuits and Systems for Video Technology*, 31(10):3736–3764, 2021.
- [10] Joaquim Campos, Simon Meierhans, Abdelaziz Djelouah, and Christopher Schroers. Content adaptive optimization for neural image compression. *arXiv preprint arXiv:1906.01223*, 2019.
- [11] Zhengxue Cheng, Heming Sun, Masaru Takeuchi, and Jiro Katto. Learned image compression with discretized

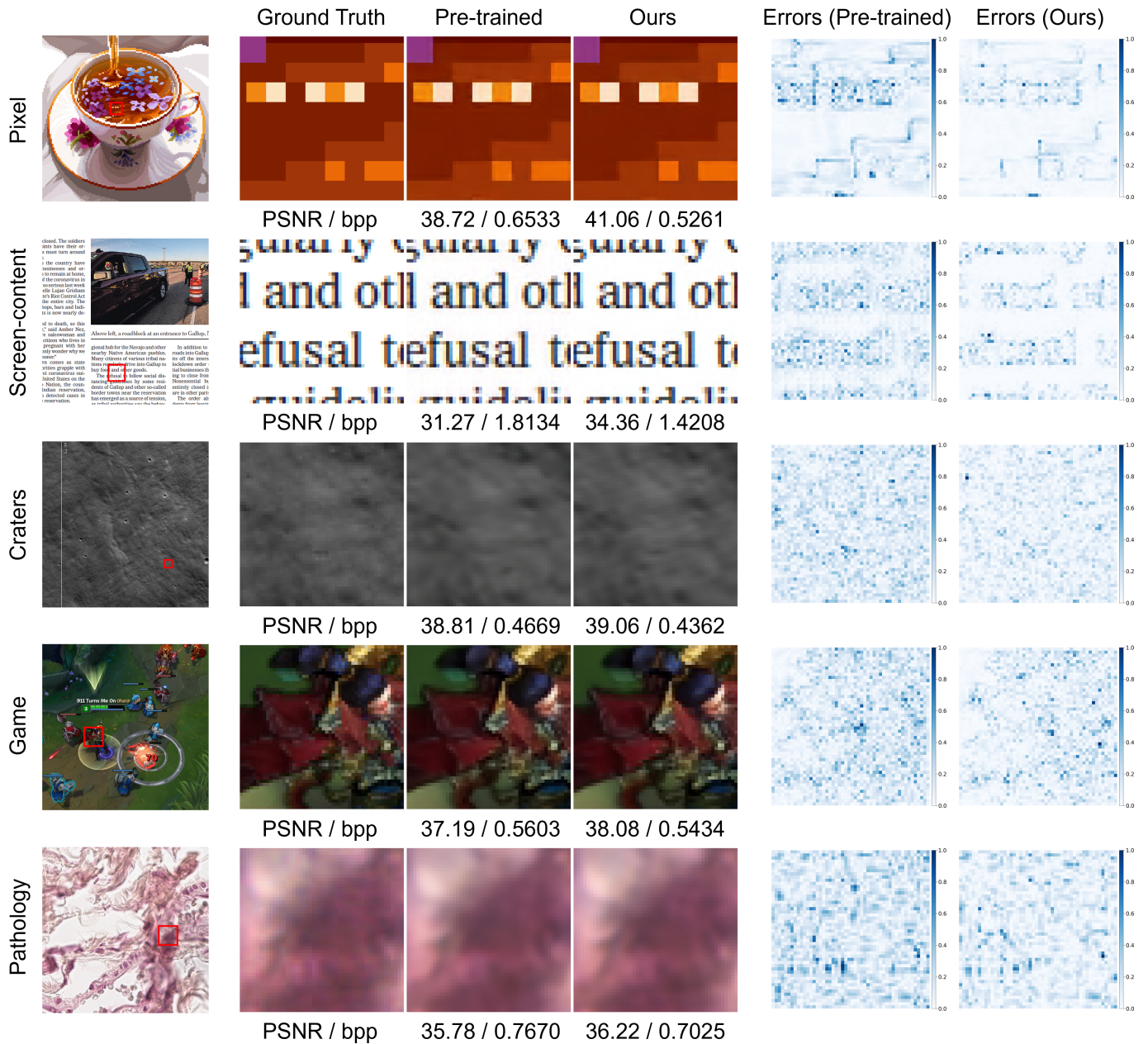


Fig. 12. Reconstructions and PSNR (\uparrow) /bpp (\downarrow) performance compared with ground truth and the pre-trained model, detailed by specific 50×50 crops. The reconstruction errors with ground truth are shown in right.

gaussian mixture likelihoods and attention modules. In *Proceedings of the IEEE/CVF conference on computer vision and pattern recognition*, pages 7939–7948, 2020.

[12] CLIC. Workshop and challenge on learned image compression. <https://www.compression.cc/>, 2020.

[13] Xin Cong, Bowen Yu, Tingwen Liu, Shiyao Cui, Hengzhu Tang, and Bin Wang. Inductive unsupervised domain adaptation for few-shot classification via clustering. In *Machine Learning and Knowledge Discovery in Databases: European Conference, ECML PKDD 2020, Ghent, Belgium, September 14–18, 2020, Proceedings, Part II*, pages 624–639. Springer, 2021.

[14] Zhihao Duan, Ming Lu, Zhan Ma, and Fengqing Zhu. Opening the black box of learned image coders. In *2022*

Picture Coding Symposium (PCS), pages 73–77. IEEE, 2022.

[15] Chelsea Finn, Pieter Abbeel, and Sergey Levine. Model-agnostic meta-learning for fast adaptation of deep networks. In *International Conference on Machine Learning*, pages 1126–1135. PMLR, 2017.

[16] Rich Franzen. Kodak lossless true color image suite (photocd pcd0992). <http://r0k.us/graphics/kodak/>, 1993.

[17] Rinon Gal, Or Patashnik, Haggai Maron, Amit H Bermano, Gal Chechik, and Daniel Cohen-Or. Stylegan-nada: Clip-guided domain adaptation of image generators. *ACM Transactions on Graphics (TOG)*, 41(4):1–13, 2022.

[18] Zongyu Guo, Zhizheng Zhang, Runsen Feng, and Zhibo

- Chen. Soft then hard: Rethinking the quantization in neural image compression. In *International Conference on Machine Learning*, pages 3920–3929. PMLR, 2021.
- [19] Dailan He, Ziming Yang, Weikun Peng, Rui Ma, Hongwei Qin, and Yan Wang. Elic: Efficient learned image compression with unevenly grouped space-channel contextual adaptive coding. In *Proceedings of the IEEE/CVF Conference on Computer Vision and Pattern Recognition*, pages 5718–5727, 2022.
- [20] Edward J Hu, Yelong Shen, Phillip Wallis, Zeyuan Allen-Zhu, Yuanzhi Li, Shean Wang, Lu Wang, and Weizhu Chen. Lora: Low-rank adaptation of large language models. *arXiv preprint arXiv:2106.09685*, 2021.
- [21] Wei Jiang and Ronggang Wang. Mlic++: Linear complexity multi-reference entropy modeling for learned image compression. In *ICML 2023 Workshop Neural Compression: From Information Theory to Applications*, 2023. URL <https://openreview.net/forum?id=hxIpcSoz2t>.
- [22] Wei Jiang, Jiayu Yang, Yongqi Zhai, Peirong Ning, Feng Gao, and Ronggang Wang. Mlic: Multi-reference entropy model for learned image compression. In *Proceedings of the 31st ACM International Conference on Multimedia*, pages 7618–7627, 2023.
- [23] Tarun Kalluri and Manmohan Chandraker. Cluster-to-adapt: Few shot domain adaptation for semantic segmentation across disjoint labels. In *Proceedings of the IEEE/CVF Conference on Computer Vision and Pattern Recognition*, pages 4121–4131, 2022.
- [24] Sudeep Katakol, Luis Herranz, Fei Yang, and Marta Mrak. Danice: Domain adaptation without forgetting in neural image compression. In *Proceedings of the IEEE/CVF Conference on Computer Vision and Pattern Recognition*, pages 1921–1925, 2021.
- [25] Marvin Klingner, Jan-Aike Termöhlen, Jacob Ritterbach, and Tim Fingscheidt. Unsupervised batchnorm adaptation (ubna): A domain adaptation method for semantic segmentation without using source domain representations. In *Proceedings of the IEEE/CVF Winter Conference on Applications of Computer Vision*, pages 210–220, 2022.
- [26] Gihyun Kwon and Jong Chul Ye. One-shot adaptation of gan in just one clip. *IEEE Transactions on Pattern Analysis and Machine Intelligence*, 2023.
- [27] Shaohua Li, Xiuchao Sui, Jie Fu, Huazhu Fu, Xiangde Luo, Yangqin Feng, Xinxing Xu, Yong Liu, Daniel SW Ting, and Rick Siow Mong Goh. Few-shot domain adaptation with polymorphic transformers. In *Medical Image Computing and Computer Assisted Intervention—MICCAI 2021: 24th International Conference, Strasbourg, France, September 27–October 1, 2021, Proceedings, Part II 24*, pages 330–340. Springer, 2021.
- [28] Shaohui Li, Wenrui Dai, Yimian Fang, Ziyang Zheng, Wen Fei, Hongkai Xiong, and Wei Zhang. Revisiting learned image compression with statistical measurement of latent representations. *IEEE Transactions on Circuits and Systems for Video Technology*, 34(4):2891–2907, 2024.
- [29] Wei-Hong Li, Xialei Liu, and Hakan Bilen. Cross-domain few-shot learning with task-specific adapters. In *Proceedings of the IEEE/CVF Conference on Computer Vision and Pattern Recognition*, pages 7161–7170, 2022.
- [30] Jinming Liu, Heming Sun, and Jiro Katto. Learned image compression with mixed transformer-cnn architectures. In *Proceedings of the IEEE/CVF Conference on Computer Vision and Pattern Recognition*, pages 14388–14397, 2023.
- [31] Zhihe Lu, Sen He, Xiatian Zhu, Li Zhang, Yi-Zhe Song, and Tao Xiang. Simpler is better: Few-shot semantic segmentation with classifier weight transformer. In *Proceedings of the IEEE/CVF International Conference on Computer Vision*, pages 8741–8750, 2021.
- [32] Yue Lv, Jinxi Xiang, Jun Zhang, Wenming Yang, Xiao Han, and Wei Yang. Dynamic low-rank instance adaptation for universal neural image compression. In *Proceedings of the 31st ACM International Conference on Multimedia*, pages 632–642, 2023.
- [33] David Minnen, Johannes Ballé, and George D Toderici. Joint autoregressive and hierarchical priors for learned image compression. *Advances in neural information processing systems*, 31:10794–10803, 2018.
- [34] Zhangkai Ni, Lin Ma, Huanqiang Zeng, Jing Chen, Canhui Cai, and Kai-Kuang Ma. Esim: Edge similarity for screen content image quality assessment. *IEEE Transactions on Image Processing*, 26(10):4818–4831, 2017.
- [35] Alberto Presta, Gabriele Spadaro, Enzo Tartaglione, Attilio Fiandrotti, and Marco Grangetto. Domain adaptation for learned image compression with supervised adapters. In *2024 Data Compression Conference (DCC)*, pages 33–42. IEEE, 2024.
- [36] Mark S Robinson, SM Brylow, M Tschimmel, D Humm, SJ Lawrence, PC Thomas, Brett W Denevi, E Bowman-Cisneros, J Zerr, MA Ravine, et al. Lunar reconnaissance orbiter camera (lroc) instrument overview. *Space science reviews*, 150:81–124, 2010.
- [37] Kate Saenko, Brian Kulis, Mario Fritz, and Trevor Darrell. Adapting visual-category models to new domains. In *Computer Vision—ECCV 2010: 11th European Conference on Computer Vision, Heraklion, Crete, Greece, September 5–11, 2010, Proceedings, Part IV 11*, pages 213–226. Springer, 2010.
- [38] Sheng Shen, Huanjing Yue, and Jingyu Yang. Dec-adapt: Exploring efficient decoder-side adapter for bridging screen content and natural image compression. In *Proceedings of the IEEE/CVF International Conference on Computer Vision*, pages 12887–12896, 2023.
- [39] Peeyush Singhal, Rahee Walambe, Sheela Ramanna, and Ketan Kotecha. Domain adaptation: Challenges, methods, datasets, and applications. *IEEE Access*, 2023.
- [40] Yisheng Song, Ting Wang, Puyu Cai, Subrota K Mondal, and Jyoti Prakash Sahoo. A comprehensive survey of few-shot learning: Evolution, applications, challenges, and opportunities. *ACM Computing Surveys*, 2023.
- [41] Gary J Sullivan, Jens-Rainer Ohm, Woo-Jin Han, and Thomas Wiegand. Overview of the high efficiency video coding (hevc) standard. *IEEE Transactions on circuits*

- and systems for video technology*, 22(12):1649–1668, 2012.
- [42] Koki Tsubota, Hiroaki Akutsu, and Kiyoharu Aizawa. Universal deep image compression via content-adaptive optimization with adapters. In *Proceedings of the IEEE/CVF Winter Conference on Applications of Computer Vision*, pages 2529–2538, 2023.
- [43] Ties Van Rozendaal, Johann Brehmer, Yunfan Zhang, Reza Pourreza, Auke Wiggers, and Taco S Cohen. Instance-adaptive video compression: Improving neural codecs by training on the test set. *arXiv preprint arXiv:2111.10302*, 2021.
- [44] Ties van Rozendaal, Iris AM Huijben, and Taco S Cohen. Overfitting for fun and profit: Instance-adaptive data compression. 2021.
- [45] Gregory K Wallace. The jpeg still picture compression standard. *Communications of the ACM*, 34(4):30–44, 1991.
- [46] Ceyuan Yang, Yujun Shen, Zhiyi Zhang, Yinghao Xu, Jiapeng Zhu, Zhirong Wu, and Bolei Zhou. One-shot generative domain adaptation. In *Proceedings of the IEEE/CVF International Conference on Computer Vision*, pages 7733–7742, 2023.
- [47] Huan Yang, Yuming Fang, and Weisi Lin. Perceptual quality assessment of screen content images. *IEEE Transactions on Image Processing*, 24(11):4408–4421, 2015.
- [48] Jingyu Yang, Sheng Shen, Huanjing Yue, and Kun Li. Implicit transformer network for screen content image continuous super-resolution. *Advances in Neural Information Processing Systems*, 34:13304–13315, 2021.
- [49] Yibo Yang, Robert Bamler, and Stephan Mandt. Improving inference for neural image compression. *Advances in Neural Information Processing Systems*, 33:573–584, 2020.
- [50] Zicheng Zhang, Yinglu Liu, Congying Han, Tiande Guo, Ting Yao, and Tao Mei. Generalized one-shot domain adaptation of generative adversarial networks. *Advances in Neural Information Processing Systems*, 35:13718–13730, 2022.
- [51] Nannan Zou, Honglei Zhang, Francesco Cricri, Ramin G Youvalari, Hamed R Tavakoli, Jani Lainema, Emre Aksu, Miska Hannuksela, and Esa Rahtu. Adaptation and attention for neural video coding. In *2021 IEEE International Symposium on Multimedia (ISM)*, pages 240–244. IEEE, 2021.